IN-SITU FORMATION AND DENSIFICATION OF $MgAl_2O_4$–$SmAlO_3$ CERAMICS BY A SINGLE-STAGE REACTION SINTERING PROCESS

[#]BEIYUE MA*, YUE YIN*, QIANG ZHU**, [##]YING LI*, GUANGQIANG LI***, JINGKUN YU*

*School of Materials and Metallurgy, Northeastern University, Shenyang 110819, China
**School of Mechanical, Materials and Mechatronic Engineering,
University of Wollongong, NSW 2522, Australia
***The State Key Laboratory of Refractories and Metallurgy,
Wuhan University of Science and Technology, Wuhan 430081, China

[#]E-mail: maby@smm.neu.edu.cn, [##]E-mail: liying@mail.neu.edu.cn

Submitted January 15, 2015; accepted May 21, 2015

Keywords: $MgAl_2O_4$–$SmAlO_3$, Sm_2O_3, Reaction sintering, Sintering properties, Strength

Stoichiometric magnesium aluminate spinel ($MgAl_2O_4$, MA)–samarium aluminate ($SmAlO_3$, SA) ceramics have been prepared at 1580°C for 4 h from calcined magnesia (MgO), commercial alumina (Al_2O_3) and samarium oxide (Sm_2O_3) by a single-stage in-situ reaction sintering (SIRS) method. The phase compositions, microstructures, shrinkage ratio, bulk density and cold compressive strength of the MA–SA ceramics have been investigated. The ceramics with 2.5 - 7.5 wt. % Sm_2O_3 are composed of MA and SA phases. The microstructures of the ceramics are dense. MA particles exist as angular shape, and their grain size varies between 2 and 10 μm but the average grain size is about 5 μm. $SmAlO_3$ particles form due to the reaction of Sm_2O_3 and Al_2O_3, and they distribute in the intergranular space of MA grains. The diameter shrinkage ratio, volume shrinkage ratio, bulk density and cold compressive strength of MA–SA ceramics are greatly improved due to the addition of Sm_2O_3.

INTRODUCTION

Magnesium aluminate spinel ($MgAl_2O_4$, MA) has increasingly attracted much attention and been extensively used for refractory materials, optical ceramics and humidity sensors due to its excellent properties including high melting point (2135°C), high hardness (16.1 GPa), high flexural strength (180 MPa), low thermal expansion coefficient (~ 9×10^{-6} °C^{-1} between 30 and 1400°C), excellent transmittance in the range of 0.25 - 5.0 μm wavelength, good chemical inertness, thermal shock resistance and corrosion resistance [1-4]. A number of methods have been developed to fabricate MA ceramics such as reaction sintering [5], hot pressing sintering [6], high pressure sintering [7], microwave sintering [8] and spark plasma sintering [9], etc., among which reaction sintering is regarded as one of the most promising processes due to its simple operation and easy access of raw materials such as magnesite and bauxite [10] for example. MA ceramics with high density are very difficultly obtained by a single-stage reaction sintering process because the formation of spinel from oxides mixture usually companies a volume expansion of about 8% during the reaction [2]. To solve this problem, a two-stage reaction sintering process is often adopted: i) the formation of spinel is completed at a lower temperature at the first stage, and then ii) a sintering (or densification) process is conducted at the second stage. However, like other synthesis process mentioned above two-stage reaction sintering process suffers from expensive production cost and complexity.

An alternative way to improve the densification of MA during the sintering process is to introduce additives such as ZrO_2 [11], Cr_2O_3 [5], Dy_2O_3 [12], Nd_2O_3 [13] and $AlCl_3$ [14]. Moreover, some additives can also improve the mechanical properties and thermal shock resistance of MA ceramics. Ganesh *et al.* [11] found that yttria partially stabilized zirconia (YPSZ) additive increases the sintering ability, fracture toughness and hardness of MA materials. Sarkar *et al.* [5] reported that Cr_2O_3 additive has the greatest effect on the densification for alumina rich MA spinel at 1550°C, and 1.0 wt. % Cr_2O_3 addition is beneficial in restricting the strength degradation after thermal shock for the stoichiometric MA spinel. Tripathi *et al.* [12] found that Dy_2O_3 additive prevents the exaggerated grain growth and favors the densification of MA. Tian *et al.* [13] reported that Nd_2O_3 additive improves spinel crystallization and is beneficial to the sintering densification of MA. Ganesh *et al.* [14] reported that $AlCl_3$ is favorable for improving the formation and sintering densification of MA ceramics.

However, up to date, there are limited works published on the spinel formation and sintering densification of MA ceramics by addition of rare earths [12, 13],

especially Sm_2O_3. In this paper, calcined MgO and commercial Al_2O_3 were used as raw materials, and Sm_2O_3 was chosen as the additive to prepare MA–$SmAlO_3$ (SA) ceramics, and the phase compositions, microstructures, shrinkage ratio, bulk density and cold compressive strength of the ceramics with 2.5 - 7.5 wt. % Sm_2O_3 additions have been investigated in detail.

EXPERIMENTAL

Preparation process

Table 1 lists raw materials for the synthesis of MA–SA ceramics. The powders of calcined MgO and commercial Al_2O_3 were weighted according to a MgO:Al_2O_3 mole ratio of 1:1. Sm_2O_3 was chosen as additive to form $SmAlO_3$ by an in-situ reaction between Sm_2O_3 and Al_2O_3, and its addition amounts were designed as 2.5, 5.0 and 7.5 wt. %. The powders containing above raw materials were fully milled for 3 h in a planetary ball mill with alcohol as the medium. The milled mixture powders were fully dried at 120°C, and then pressed at 200 MPa to form samples with dimension of 15 mm in diameter and 12 mm in height. All the formed samples were placed in a high temperature resistance furnace and sintered at 1580°C for 4 h.

Composition, microstructure and property characterization

The phase compositions of as-prepared MA–SA samples were characterized by X-ray diffraction (XRD, Cu Kα radiation, 30 kV and 30 mA). International Center for Diffraction Data (ICDD) cards used for identification were spinel (MA, 01–082–2424, 01–075–1797) and $SmAlO_3$ (00–052–1519, 00–029–0082). The microstructures and element distributions of as-prepared MA–SA samples were examined and scanning electron microscope (SEM) and energy dispersive spectroscopy (EDS).

In this paper, sintering properties including diameter shrinkage ratio, volume shrinkage ratio and bulk density of MA–SA samples were studied. The diameter shrinkage ratio and volume shrinkage ratio were calculated based on the Equations 1 and 2. The bulk density was measured in water under vacuuming condition using Archimedes' principle, and was calculated by Equation 3 [15].

$$\Delta D = \frac{D_0 - D_1}{D_0} \times 100\% \quad (1)$$

$$\Delta V = \frac{D_0^2 H_0 - D_1^2 H_1}{D_0^2 H_0} \times 100\% \quad (2)$$

$$D_b = \frac{m_1 d}{m_3 - m_2} \quad (3)$$

where ΔD and ΔV are the diameter shrinkage ratio and volume shrinkage ratio of as-sintered samples (%), D_b is the bulk density of as-sintered samples ($g \cdot cm^{-3}$), D_0 and H_0 are the diameter and height of the samples before sintering (mm), D_1 and H_1 are the diameter and height of the samples after sintering (mm), m_1 is the mass of a dried sample in air (g), m_2 is the mass of the sample in water (g), m_3 is the mass of the sample with free bubbles on the surface (g), and d is the density of water ($g \cdot cm^{-3}$).

The cold compressive strength of MA-SA samples was measured using a CMT5105 type universal tester with loading rate of 0.5 $mm \cdot min^{-1}$. The sample size was φ 15 mm × 12 mm. The cold compressive strength (*CS*) was calculated by Equation 4 [16].

$$CS = \frac{P}{A} \quad (4)$$

where *CS*, *P* and *A* represent the cold compressive strength (MPa), maximum load of sample damage (N) and sample compressive area (mm^2), respectively.

RESULTS AND DISCUSSION

Phase compositions

Figure 1 shows XRD diffraction patterns of as-synthesized MA–SA ceramics at 1580°C for 4 h. The XRD analysis shows that MgO and Al_2O_3 phases can not be detected after sintering, which means that MgO fully reacted with Al_2O_3 and completely formed $MgAl_2O_4$. It was also found that a new phase $SmAlO_3$ formed, which indicates that there was a chemical reaction occurring between Sm_2O_3 and Al_2O_3 during the sintering process. With increasing amounts of Sm_2O_3 additive from 2.5 up

Table 1. Raw materials for the synthesis of MA–SA ceramics.

Raw materials	Chemical compositions (wt. %)			Particle size (μm)	Production place
	MgO	Al_2O_3	Sm_2O_3		
Calcined MgO	99	–	–	74	Liaoning Yingkou Qinghua Group Co. Ltd., China
Commercial Al_2O_3	–	99	–	44	Henan Xingyang Tenai Grinding Materials Co. Ltd., China
Chemical reagent Sm_2O_3	–	–	99.9	–	Sinopharm Chemical Reagent Co. Ltd, China

to 7.5 wt. %, the diffraction intensity of $SmAlO_3$ increases (Figure 1a-c). Based on the Al_2O_3–Sm_2O_3–ZrO_2 phase diagram, the $SmAlO_3$ and $Sm_4Al_2O_9$ compounds are formed at 1250 and 1650°C [17]. In this study, the $Sm_4Al_2O_9$ compound can not be produced due to small amount of Sm_2O_3 additive (2.5 - 7.5 wt. %) in sample.

The reactions of MgO and Sm_2O_3 with Al_2O_3 to synthesize $MgAl_2O_4$ and $SmAlO_3$ are shown in Equations 5 and 6. The expression between standard Gibbs free energy (ΔG^θ) and temperature (T, K) of reaction (5) is as below [18].

$$MgO(s) + Al_2O_3(s) = MgAl_2O_4(s) \quad (5)$$

$$Sm_2O_3(s) + Al_2O_3(s) = SmAlO_3(s) \quad (6)$$

$$\Delta G^\theta_5\ (J\cdot mol^{-1}) = -35\,600 - 2.09T\ (K) \quad (7)$$

In this study, sintering temperature was set as 1580°C (T = 1853 K), therefore ΔG^θ_5 is calculated as –39 472.77 $J\cdot mol^{-1}$. It reveals that the thermodynamic requirement for producing $MgAl_2O_4$ from MgO and Al_2O_3 is fully satisfied.

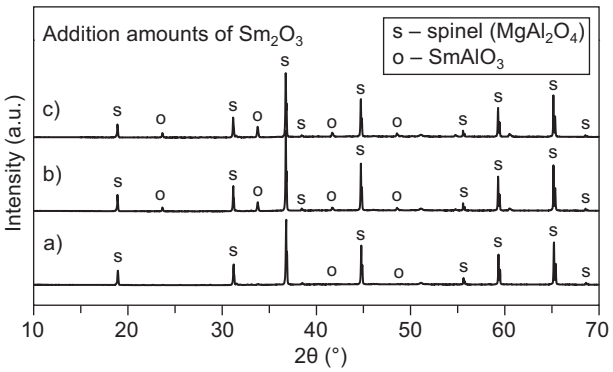

Figure 1. XRD patterns of the $MgAl_2O_4$–$SmAlO_3$ ceramics prepared at 1580°C for 4 h and doped with a) 2.5, b) 5.0 and c) 7.5 wt. % Sm_2O_3.

Microstructures and elements distributions

Figure 2 shows SEM images of as-prepared MA-SA ceramics at 1580°C for 4 h. It can be seen that there is no obvious porosity existing in the microstructure of MA–SA ceramics. It was observed that there exist gray and big particles as well as white and small particles or cotton-like material. The gray and big particles have an angular shape, and their grain size varies between 2 and 10 μm but the average grain size is about 5 μm. The average grain size of white and small particles is about 2 μm.

Figure 3 shows EDS spectrums of MA-SA ceramics doped with 2.5 – 7.5 wt. % Sm_2O_3 and sintered at 1580°C for 4 h. EDS analysis shown in Figure 3a indicates that white and small particle (zone A) consists of Al, Mg, O and Sm elements, and gray and big particle (zone A') is composed of Al, Mg and O elements. Combining with XRD patterns shown in Figure 1, zone A and A' are $SmAlO_3$ and $MgAl_2O_4$, respectively. It can be seen from Figure 3b that cotton-like material (zone B) is mainly composed of Al, Mg, O and Sm elements, and zone B is $SmAlO_3$. In Figure 3c white particle C mainly consists of Al, O and Sm elements, and zone C is $SmAlO_3$.

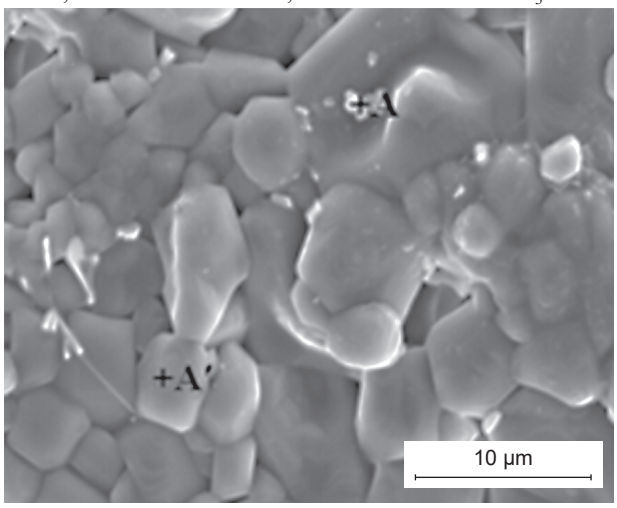

a) 2.5 wt. %

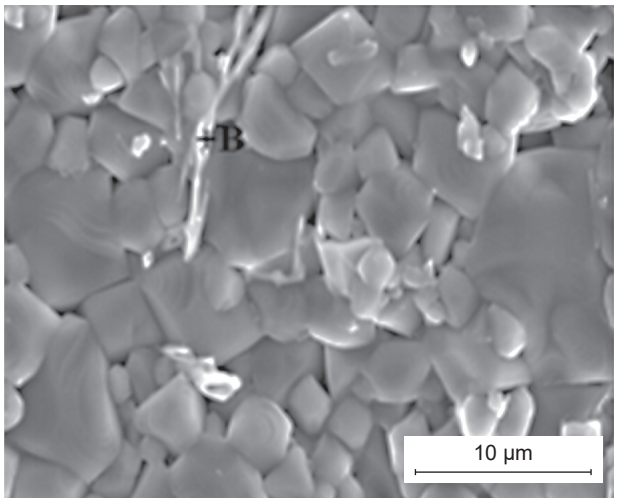

b) 5.0 wt. %

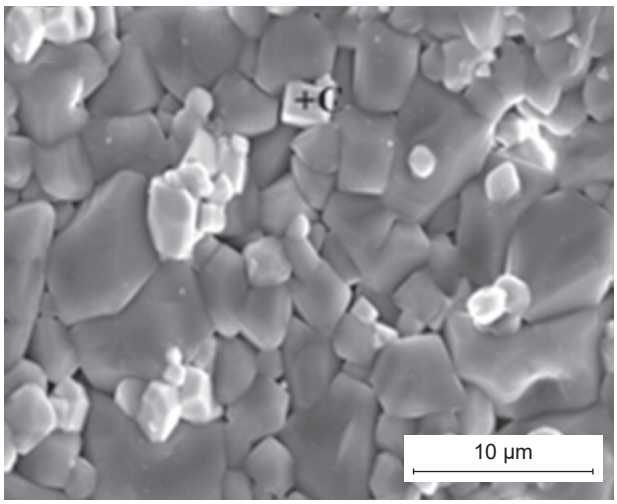

c) 7.5 wt. %

Figure 2. SEM images of the $MgAl_2O_4$–$SmAlO_3$ ceramics prepared at 1580°C for 4 h and doped with a) 2.5, b) 5.0 and c) 7.5 wt. % Sm_2O_3.

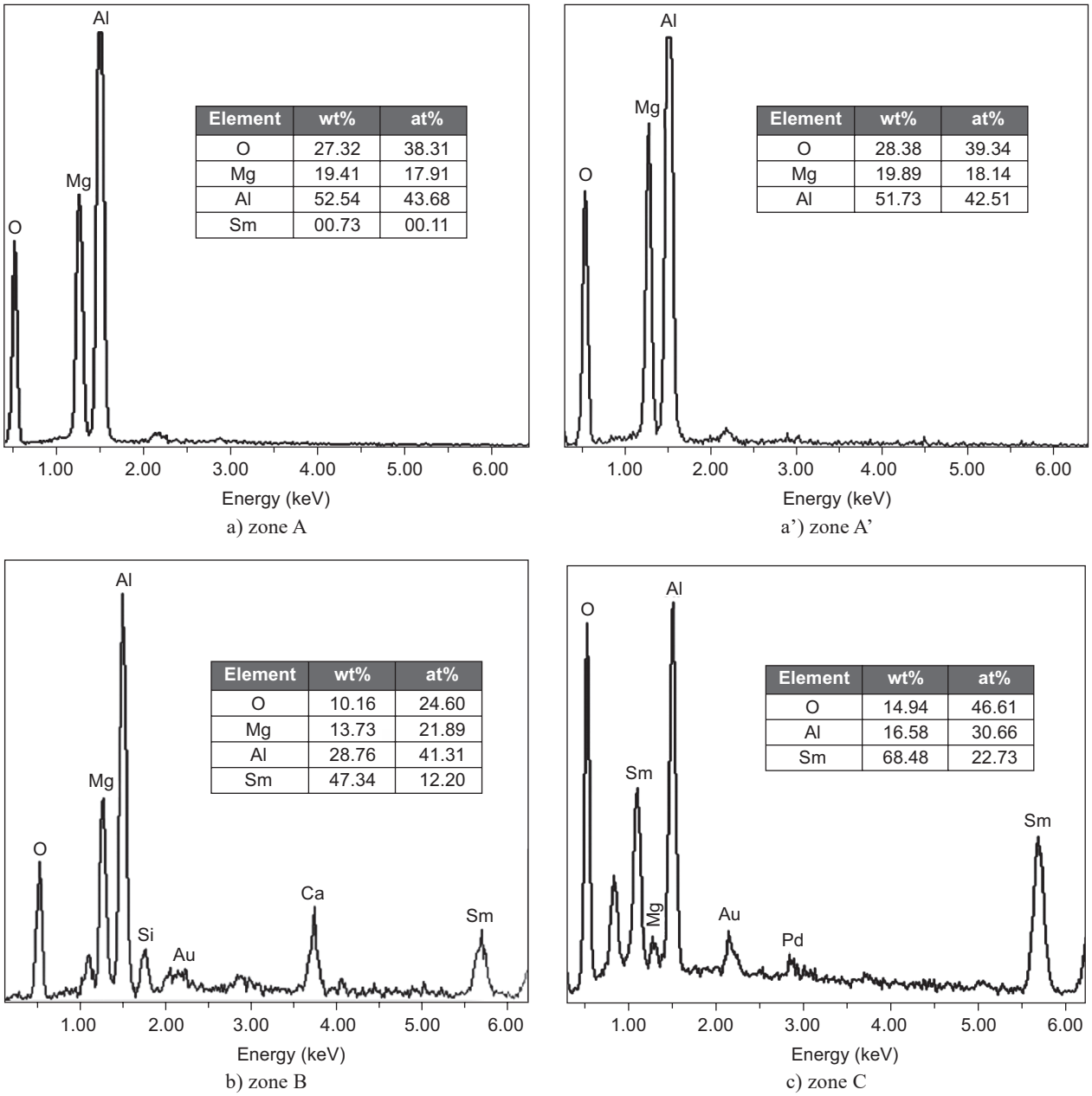

Figure 3. EDS spectrums of zones A, A', B and C shown in Figure 2: a) zone A, a') zone A', b) zone B and c) zone C.

It is important noted that Mg shown in Figure 3a and b possibly derives from the MA matrix element. During the EDS analysis, the spot size of electron beam is quite large, probably greater than 1 μm in dimension, it is rather like a small area analysis than a spot. When the particle shown in Figure 3a and b is too small, the surrounding matrix will lead to the detection of Mg element. Thus, zones A and B are concluded be $SmAlO_3$. Moreover, Ca and Si elements shown in Figure 3b are possibly from raw materials, Au and Pd shown in Figure 3c can be observed due to the metal coating of the samples used for SEM characterization.

It can also be observed from Figure 2 that the formed $SmAlO_3$ particles are mainly present in the intergranular space and grain boundaries of MA particles.

Sintering properties and cold compressive strength

Figure 4 shows diameter shrinkage ratio and volume shrinkage ratio of MA–SA ceramics doped with 2.5 - 7.5 wt. % Sm_2O_3 and sintered at 1580°C for 4 h. It is clearly observed that MA–SA samples with 2.5 - 7.5 wt. % Sm_2O_3 additions have high shrinkage ratios. With increasing the additive amount of Sm_2O_3, the diameter shrinkage ratio and volume shrinkage ratio of the samples gradually increase. The diameter shrinkage ratio and volume shrinkage ratio of the sample added with 2.5 wt. % Sm_2O_3 are 10.57 % and 28.17 %, respectively. For the sample by addition of 5.0 wt. % Sm_2O_3, its diameter shrinkage ratio and volume shrinkage ratio

increase to 11.12 % and 29.10 %, respectively. When 7.5 wt. % Sm_2O_3 was doped, the diameter shrinkage ratio and volume shrinkage ratio achieve their maximum values of 11.25 % and 29.76 %, respectively.

Figure 5 shows change curves of bulk density and cold compressive strength of MA–SA ceramics doped with various amounts of Sm_2O_3 and sintered at 1580°C for 4 h. It was clearly found that the MA–SA samples with 2.5 – 7.5 wt. % Sm_2O_3 additions have high bulk density and cold compressive strength. With increasing addition amounts of Sm_2O_3 ranging from 2.5 wt. % to 5.0 wt. %, the bulk density gradually increases from 3.07 to 3.12 g·cm^{-3}, and the strength increases from 197.9 to 198.9 MPa. The sample doped with 7.5 wt. % Sm_2O_3 gets its maximum density of 3.13 g·cm^{-3}, and has maximum strength of 209.4 MPa. To some extent the formed $SmAlO_3$ particles occupy the grain boundary position (Figure 2), inhibit the grain growth of MA, and they can further improve the density of MA ceramics [12]. The in-situ formed $SmAlO_3$ from Sm_2O_3 and Al_2O_3 partly contributes to the increase of cold compressive strength of MA–SA ceramics. Additional detailed research and characterization need to be performed to fully understand the reason on how to increase the strength due to the addition of Sm_2O_3. It is concluded from Figures 4 and 5 that Sm_2O_3 additive favors to improve the diameter shrinkage ratio, volume shrinkage ratio, bulk density and cold compressive strength of MA–SA ceramics.

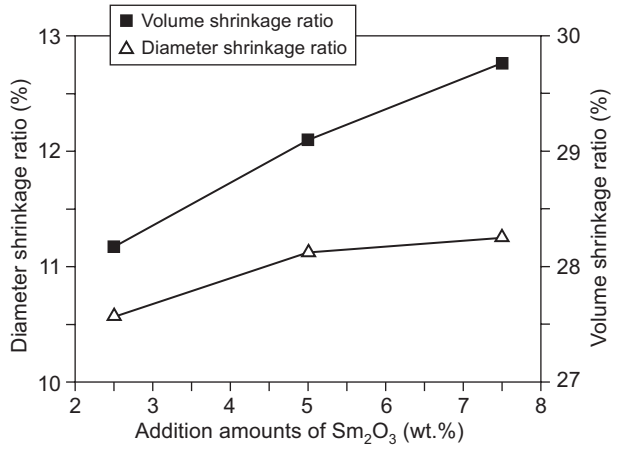

Figure 4. Change curves of diameter shrinkage ratio and volume shrinkage ratio of MA–SA ceramics prepared at 1580°C for 4 h versus addition amounts of Sm_2O_3.

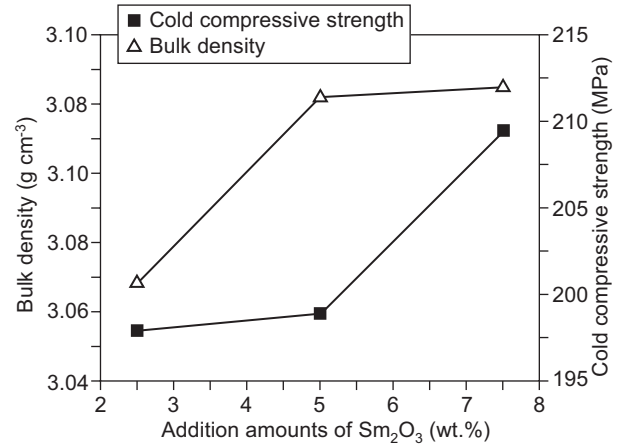

Figure 5. Change curves of bulk density and cold compressive strength of MA–SA ceramics prepared at 1580°C for 4 h versus addition amounts of Sm_2O_3.

CONCLUSIONS

- Dense $MgAl_2O_4$–$SmAlO_3$ ceramics have been successfully prepared at 1580°C for 4 h by the single-step in-situ reaction sintering method.
- $MgAl_2O_4$ and $SmAlO_3$ are formed due to the reactions of MgO and Al_2O_3 as well as Sm_2O_3 and Al_2O_3. $MgAl_2O_4$ particles have an angular shape, and their grain size varies between 2 and 10 μm but the average grain size is about 5 μm. $SmAlO_3$ particles form due to the reaction of Sm_2O_3 and Al_2O_3, and they distribute in the intergranular space of MA grains.
- With increasing the addition amounts of Sm_2O_3, the sintering properties and post-sintering properties of $MgAl_2O_4$–$SmAlO_3$ ceramics all improve gradually. The $MgAl_2O_4$–$SmAlO_3$ ceramics with 7.5 wt. % Sm_2O_3 addition achieve their maximum diameter shrinkage ratio, volume shrinkage ratio, bulk density and cold compressive strength, 11.25 %, 29.76 %, 3.13 g·cm^{-3} and 209.4 MPa, respectively.

Acknowledgments

The authors gratefully acknowledge the support of the open research fund for the State Key Laboratory of Refractories and Metallurgy of WUST (Grant No. G201402), the Fundamental Research Funds for the Central Universities (Grant No. N120402006) and National Natural Science Foundation of China (Grant No. 51474057).

REFERENCES

1. Zhang S.W., Jayaseelan D.D., Bhattacharya G., Lee W. E.: J. Am. Ceram. Soc. *89*, 1724 (2006).
2. Ganesh I.: Adv. Appl. Ceram. *110*, 496 (2011).
3. Naghizadeh R., Rezaie H.R., Golestani-Fard F.: Ceram. Int. *37*, 349 (2011).
4. Rufner J. F., Castro R.H.R., Holl T.B., Benthem K.: Acta Mater. *69*, 187 (2014).
5. Sarkar R., Das S. K., Banerjee G.: J. Eur. Ceram. Soc. *22*, 1243 (2002).
6. Aksel C., Rand B., Riley F.L., Warren P.D.: J. Eur. Ceram. Soc. *22*, 745 (2002).

7. Zaki Z.I., Mostafa N.Y., Rashad M.M.: Ceram. Int. *38*, 5231 (2012).
8. Gómez I., Hernández M., Aguilar J., Hinojosa M.: Ceram. Int. *30*, 893 (2004).
9. Morita K., Kim B.N., Yoshida H., Hiraga K.: Scripta Mater. *63*, 565 (2010).
10. Cunha-Duncan F.N., Bradt R.C.: J. Am. Ceram. Soc. *85*, 2995 (2002).
11. Ganesh I., Ferreira J.M.F.: Ceram. Int. *35*, 259 (2009).
12. Tripathi H.S., Singla S., Ghosh A.: Ceram. Int. *35*, 2541 (2009).
13. Tian Z.K., Wang Z.F., Wang X.T., Zhang B.G.: J. Wuhan Univ. Sci. Technol. (in Chinese) *31*, 377 (2008).
14. Ganesh I., Bhattacharjee S., Saha B.P., Johnson R., Mahajan Y.R.: Ceram. Int. *27*, 773 (2001).
15. Ma B.Y., Li Y., Cui S.G., Zhai Y.C.: T. Nonferr. Metal. Soc. *20*, 2331 (2010).
16. Ma B.Y., Li Y., Liu G.Q., Liang D.D.: Ceram. Int. *41*, 3237 (2015).
17. Lakizaw S., Lopato L.: J. Am. Ceram. Soc. *89*, 3516 (2006).
18. Ma B.Y., Zhu Q., Sun Y., Yu J.K., Li Y.: J. Mater. Sci. Technol. *26*, 715 (2010).